Electronic Supplementary Material (ESI) for Dalton Transactions.

Supporting Information

Metal-Organic Frameworks Derived Nitrogen-doped Carbon-Confined $CoSe_2$ Anchored on Multiwall Carbon Nanotube Networks as Anode for High-rate Sodium-ion Batteries

*Lei Chen[1], Xuefan Wang[1], Yijiao Ding[1], Yuke Li[1,2], Shi-Bin Ren[*1], Mao Shen[1], Yu-Xiang Chen[1], Wei Li [1], and De-Man Han[**1]*

[1] School of Pharmaceutical Chemical and Materials Engineering, Taizhou University, Taizhou, 318000, P. R. China

[2] Department of Chemistry, Zhejiang Sci-Tech University, Hangzhou, 310018, P. R. China

*Corresponding author.

E-mail address: renshibin@tzc.edu.cn; hdm@tzc.edu.cn.

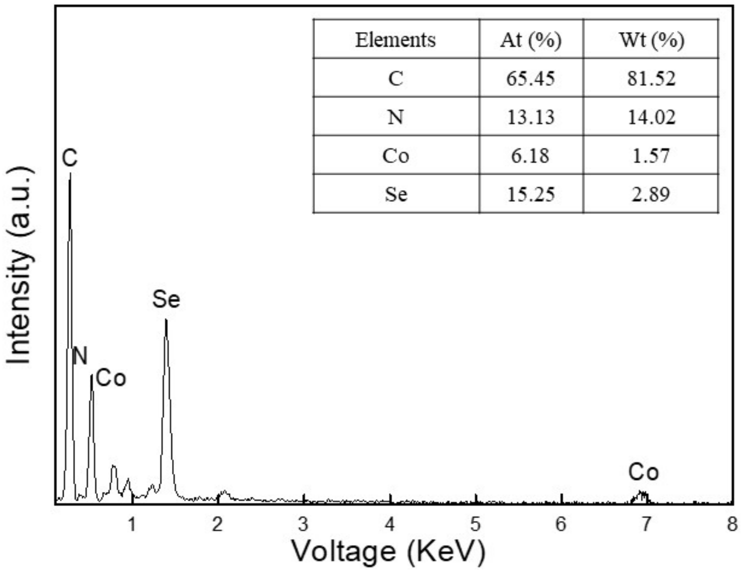

Elements	At (%)	Wt (%)
C	65.45	81.52
N	13.13	14.02
Co	6.18	1.57
Se	15.25	2.89

Figure S1. EDS spectrum of $CoSe_2$@NC/MWCNTs (the inset table is atomic and weight ratios of Co, Se, N and C in $CoSe_2$@NC/MWCNTs composite).

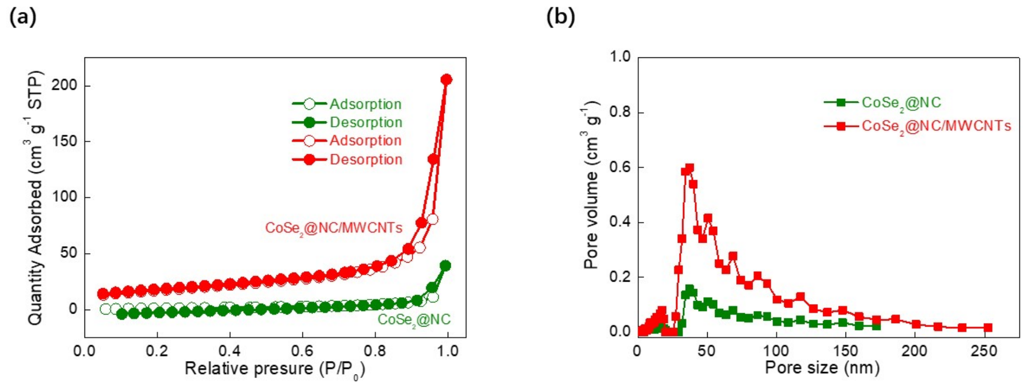

Figure S2. The nitrogen adsorption-desorption isotherms (a) and pore size distributions (b) of $CoSe_2$@NC and $CoSe_2$@NC/MWCNTs composites.

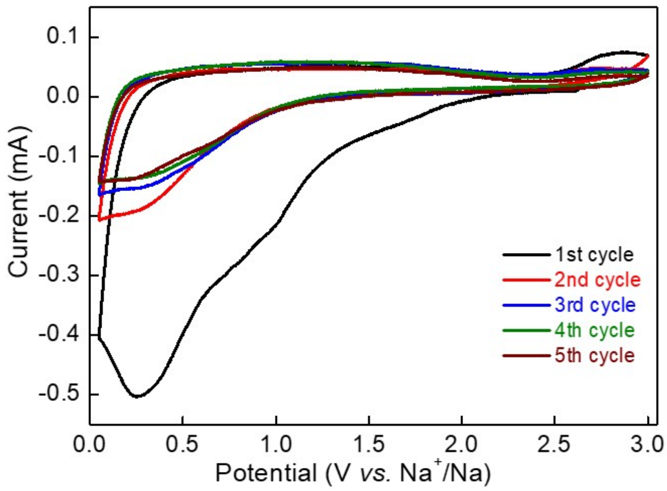

Figure S3. CV curves of the $CoSe_2$@NC electrode at scan rate of 0.2 mV s^{-1} for the initial fifth cycles.

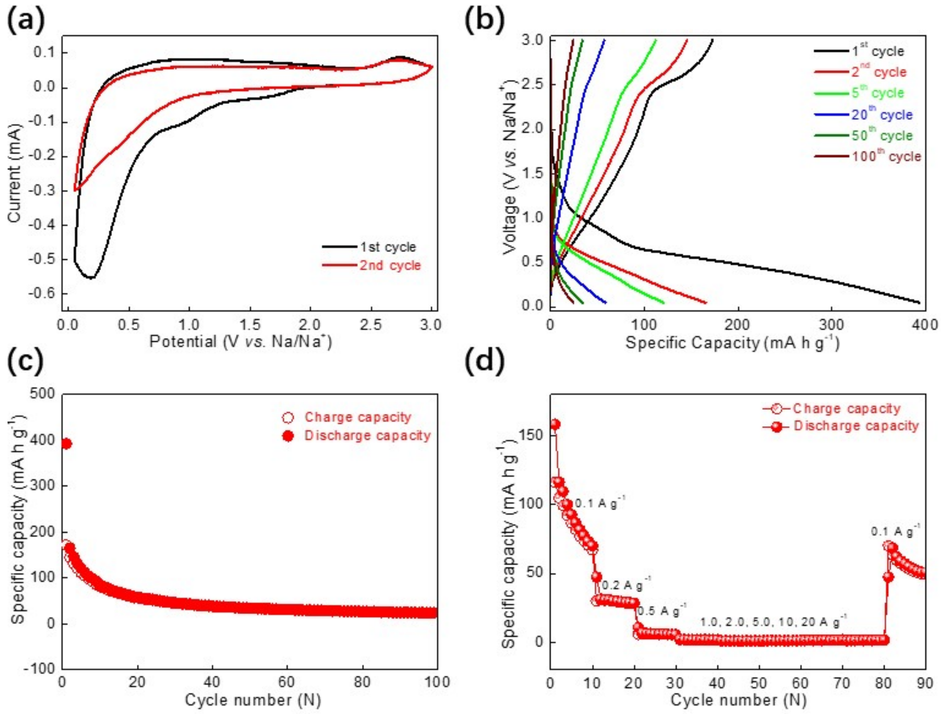

Figure S4. Electrochemical performance of Co@NC electrodes in the voltage window 0.05-3.0 V (V *vs*. Na/Na^+): (a) CV curves at scan rate of 0.1 mV s^{-1} for the initial three cycles; (b) Galvanostatic discharge/charge profiles of 1st, 2nd, 5th, 20th, 50th and 100th cycles at a current density of 0.1A g^{-1}; (c) Cycling performance at 0.1A g^{-1} over 100 cycles; (d) Rate capability at different current densities of 0.1, 0.2, 0.5, 1.0, 2.0, 5.0, 10 and 20 A g^{-1}.

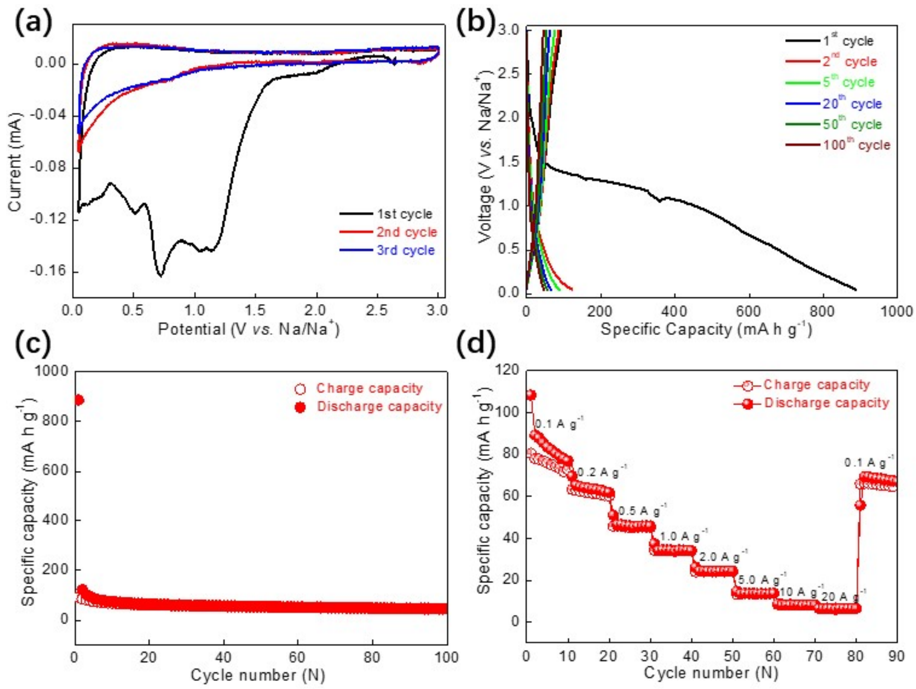

Figure S5. Electrochemical performance of MWCNTs electrodes in the voltage window 0.05-3.0 V (V *vs.* Na/Na$^+$): (a) CV curves at scan rate of 0.1 mV s^{-1} for the initial three cycles; (b) Galvanostatic discharge/charge profiles of 1st, 2nd, 5th, 20th, 50th and 100th cycles at a current density of 0.1A g^{-1}; (c) Cycling performance at 0.1A g^{-1} over 100 cycles; (d) Rate capability at different current densities of 0.1, 0.2, 0.5, 1.0, 2.0, 5.0, 10 and 20 A g^{-1}.

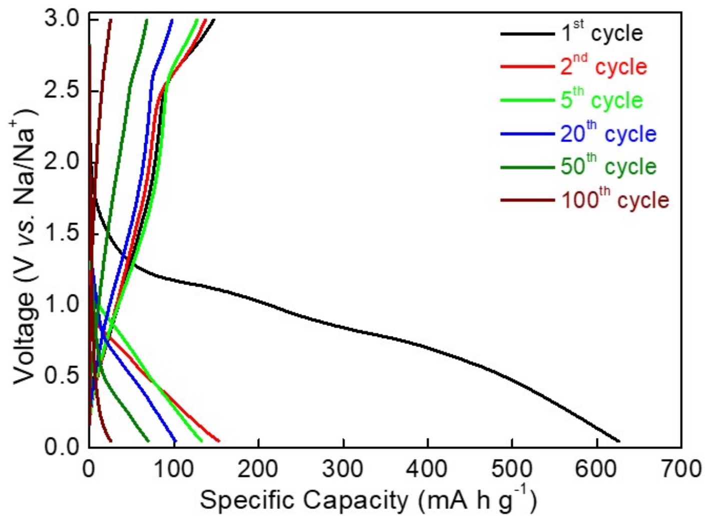

Figure S6. Galvanostatic discharge/charge profiles of the 1st, 2nd, 5th, 20th, 50th and 100th cycles for $CoSe_2$@NC electrode at a current density of 0.2 A g^{-1}.

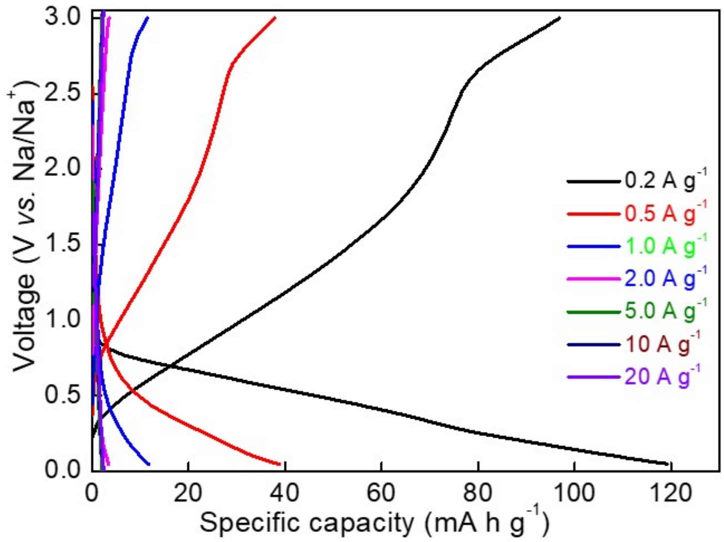

Figure S7. The charge/discharge profiles of $CoSe_2$@NC at the various current densities.

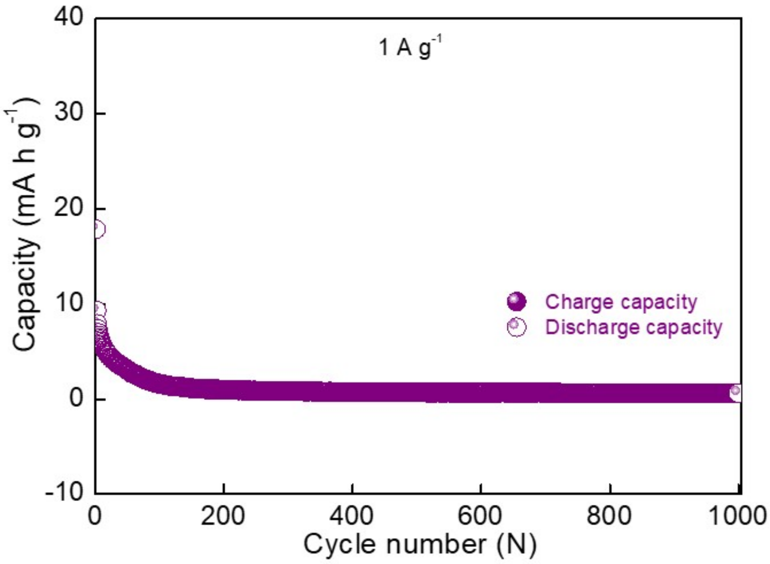

Figure S8. The long-cycling performance of $CoSe_2$@NC electrode at 1.0A g^{-1} over 1000 cycles.

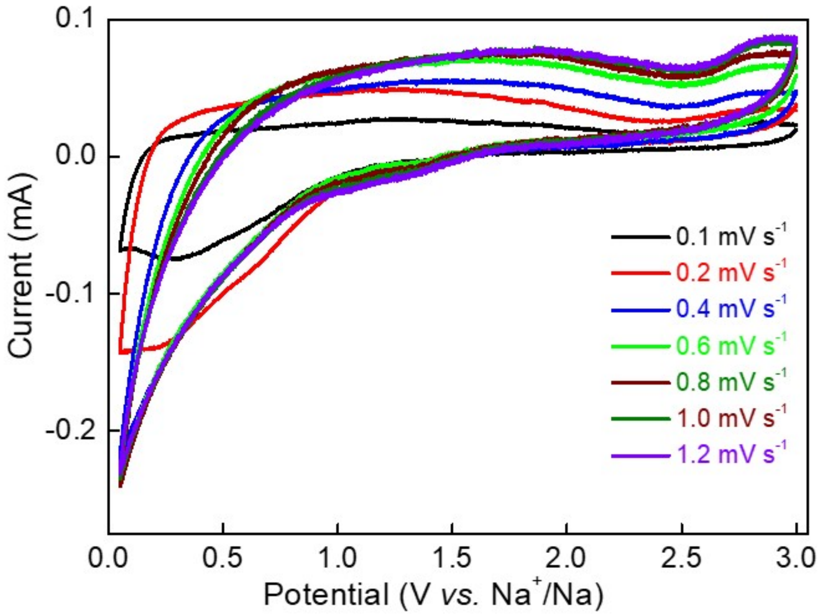

Figure S9. CV curves of $CoSe_2$@NC electrode at various scan rates from 0.1 to 1.2 mV s^{-1}.

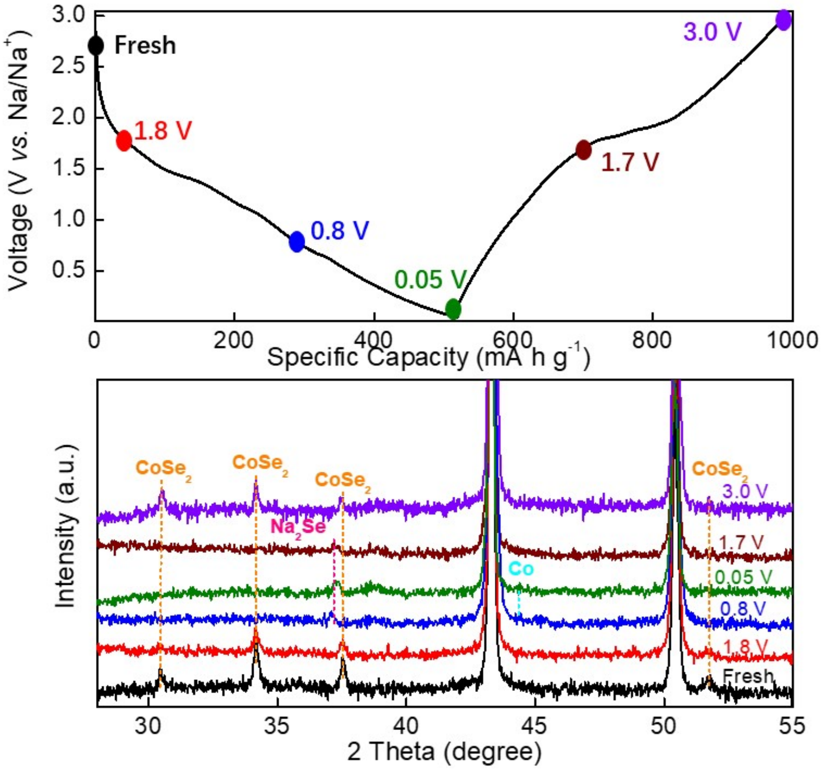

Figure S10. Ex-situ XRD analysis of the $CoSe_2$@NC/MWCNTs electrode at different charge-discharge states.

Table S1. Elemental composition of $CoSe_2$@NC/MWCNTs determined from XPS result.

Element	**Peak** (eV)	**Height**	**FWHM** (eV)	**Atomic (%)**
C1s	284.8	58711.08	0.82	94.36
Co2p	781.23	3084.39	3.09	0.54
Se3d	55.99	445.16	1.33	1.04
N1s	399.09	2177.8	1.2	4.04

Table S2. Comparison of the electrochemical performance of $CoSe_2$@NC/MWCNTs composite with previously reported $CoSe_2$-based anode for SIBs.

Samples	**Initial Capacity ($mA\ h\ g^{-1}$)**	**Long-cycling performance**	**Rate property ($mA\ h\ g^{-1}$)**	**Ref.**
$CoSe_2$@N-CA	496 (0.2 A g^{-1})	373 at 3.0 A g^{-1} (2000 cycles)	337 (10 A g^{-1})	**S1**
$CoSe_2$@NC/MX	462 (0.5 A g^{-1})	317 at 0.5 A g^{-1} (200 cycles)	343 (7 A g^{-1})	**S2**
N-$CoSe_2$ yss	602.3 (0.2 A g^{-1})	500 at 10 A g^{-1} (1000 cycles)	431 (50 A g^{-1})	**S3**
$CoSe_2$-CNS	535 (0.2 A g^{-1})	250 at 10 A g^{-1} (2000 cycles)	352 (10 A g^{-1})	**S4**
$CoSe_2$@C∩NC	389 (0.1 A g^{-1})	234 at 5 A g^{-1} (2000 cycles)	146 (25 A g^{-1})	**S5**
$CoSe_2$@NC	356 (0.2 A g^{-1})	384.3 at 2 A g^{-1} (1800 cycles)	276.4 (5 A g^{-1})	**S6**
$CoSe_2$/N-CNF	371.8 (0.2 A g^{-1})	308 at 2 A g^{-1} (1000 cycles)	295.1 (2 A g^{-1})	**S7**
$CoSe_2$/NC	541 (0.1 A g^{-1})	390.5 at 5 A g^{-1} (4000 cycles)	376.5 (10 A g^{-1})	**S8**
N-CNT/rGO/$CoSe_2$ NF	531 (0.5 A g^{-1})	264 at 10 A g^{-1} (10000 cycles)	151 (20 A g^{-1})	**S9**
$CoSe_2$@NC-NR/CNT	699 (0.2 A g^{-1})	555 at 0.2 A g^{-1} (100 cycles)	517 (5 A g^{-1})	**S10**
CNT-$CoSe_2$@NC	461.7 (0.2 A g^{-1})	404 at 0.2 A g^{-1} (120 cycles)	363 (5 A g^{-1})	**S11**
CNT/$CoSe_2$/C	531 (0.1 A g^{-1})	396 at 0.5 A g^{-1} (300 cycles)	223.6 (2.4 A g^{-1})	**S12**
$CoSe_2$@C/CNTs	470 (0.2 A g^{-1})	390 at 1 A g^{-1}	373 (10 A g^{-1})	**S13**

		(1000 cycles)		
$CoSe_2$@NC/MWCNTs	**479.6 (0.2 A g^{-1})**	**131.5 at 5 A g^{-1} (5000 cycles)**	**227.3 mA h g^{-1} at 20 A g^{-1}**	**This work**

Table S3. The calculated values of the equivalent circuit components for both samples.

Samples	R_e (Ω)	R_{SEI} (Ω)	CPE_1 (F)	R_{ct} (Ω)	CPE_2 (F)
$CoSe_2$@NC	9.59	418.9	9.74×10^{-6}	27.6	1.55×10^{-5}
$CoSe_2$@NC/MWCNTs	21.13	19.05	3.29×10^{-3}	39.8	2.59×10^{-5}

Table S4. Values of the equivalent circuit components for $CoSe_2$@NC/MWCNTs at different states.

Status	R_e (Ω)	R_s (Ω)	CPE_1 (F)	R_{ct} (Ω)	CPE_2 (F)
OCV	13.23	291.9	5.04×10^{-6}	7.9	2.44×10^{-5}
D to 1.1 V	9.494	433.5	4.26×10^{-6}	157.6	3.06×10^{-5}
D to 0.8 V	7.395	487.1	3.36×10^{-6}	141.9	8.21×10^{-5}
D to 0.05 V	9.32	276.4	5.83×10^{-6}	144.1	2.09×10^{-5}
C to 1.8 V	13.79	148.9	6.50×10^{-6}	19.19	6.97×10^{-6}
C to 2.1 V	10.47	143.2	7.52×10^{-6}	13.92	2.93×10^{-6}
C to 3.0 V	12.19	105.6	5.40×10^{-4}	20.99	4.74×10^{-6}

References

(S1) Y. Pan, X. Cheng, M. Gao, Y. Fu, J. Feng, L. Gong, H. Ahmed, H. Zhang, V. S. Battaglia, ACS Appl. Mater. Interfaces, 2020, **12**, 33621-33630.

(S2) H. G. Oh, S. H. Yang, Y. C. Kang, S.-K. Park, Int J Energy Res., 2021, **45**, 17738-17748.

(S3) J. Geng, S. Zhang, E. H. Ang, J. Guo, Z. Jin, X. Li, Y. Cheng, H. Dong, H. Geng, Mater. Chem. Front., 2021, **5**, 6873-6882.

(S4) B. Wang, X. Miao, H. Dong, X. Ma, J. Wu, Y. Cheng, H. Geng, C. C. Li, J. Mater. Chem. A, 2021, **9**, 14582.

(S5) B. Li, Y. Liu, X. Jin, S. Jiao, G. Wang, B. Peng, S. Zeng, L. Shi, J. Li and G.

Zhang, Small, 2019, **15**, 1902881.

(S6) T. Liu, Y. Li, S. Hou, C. Yang, Y. Guo, S. Tian and L. Zhao, Chem.-Eur. J., 2020, **26**, 13716-13724.

(S7) C. Cui, Z. Wei, G. Zhou, W. Wei, J. Ma, L. Chen and C. Li, J. Mater. Chem. A, 2018, **6**, 7088-7098.

(S8) H. Ge, S. Fan, J. Liu, G. Li, Energy Technol. 2021, **9**, 2001074.

(S9) M. S. Jo, J. S. Lee, S. Y. Jeong, J. K. Kim, Y. C. Kang, D. W. Kang, S. M. Jeong, J. S. Cho, Small, 2020, **16**, 2003391

(S10) S.-K. Park, Y. C. Kang, ACS Appl. Mater. Interfaces, 2018, **10**, 17203-17213.

(S11) S. H. Yang, S.-K. Park, Y. C. Kang, Chem. Eng. J., 2019, **370**, 1008-1018.

(S12) M. Yousaf, Y. Chen, H. Tabassum, Z. Wang, Y. Wang, A. Y. Abid, A. Mahmood, N. Mahmood, S. Guo, R. P. S. Han, P. Gao, Adv.Sci., 2020, **7**, 1902907.

(S13) Y. Tang, Z. Zhao, X. Hao, Y. Wang, Y. Liu, Y. Hou, Q. Yang, X. Wang, J. Qiu, J. Mater. Chem. A, 2017, **5**, 13591.